GEORGE C. MARSHALL SPACE FLIGHT CENTER

HUNTSVILLE, ALABAMA

G. B. Zerlaut and A. C. Krupnick

October 5, 1960 (NASA TM X-50722; MSFC MTP-M-S&M-M-60-6)
43p 10 refs

A NOVEL INTEGRATING SPHERE REFLECTOMETER FOR THE DETERMINATION OF ABSOLUTE HEMISPHERICAL SPECTRAL REFLECTANCE BETWEEN 0.2 AND 2.5 MICRONS (THE SOLAR SPECTRUM)

NASA

NATIONAL AERONAUTICS AND SPACE ADMINISTRATION

October 5, 1960

MTP-M-S&M-M-60-6

A NOVEL INTEGRATING SPHERE REFLECTOMETER FOR THE DETERMINATION OF ABSOLUTE HEMISPHERICAL SPECTRAL REFLECTANCE BETWEEN 0.2 AND 2.5 MICRONS (THE SOLAR SPECTRUM)

by

G. A. ZERLAUT AND A. C. KRUPNICK

ENGINEERING MATERIALS BRANCH
STRUCTURES AND MECHANICS DIVISION
GEORGE C. MARSHALL SPACE FLIGHT CENTER
NATIONAL AERONAUTICS AND SPACE ADMINISTRATION
HUNTSVILLE, ALABAMA

ACKNOWLEDGMENT

The authors wish to acknowledge the work of Mr. Julius E. Ray, Development Shop Section, Propulsion and Mechanics Branch, Structures and Mechanics Division, for the excellent precision machining of the integrating sphere used in this study.

ABSTRACT

This report describes an instrument for the measurement of the absolute hemispherical spectral reflectance of surfaces. The novelty of the instrument is the dual ability to measure and monitor the absolute reflectance of a magnesium oxide standard and to compare this reflectance to that of any other surface. The major error in the absolute methods of previous investigators may be the inability to insure that the magnesium oxide standard and the magnesium oxide smoked sphere wall possess exactly the same reflectance. This error has been essentially eliminated by designing the integrating sphere such that the reflectance of the sphere wall can be measured in terms of the standard, or conversely. The determination of the absolute reflectance of the standard can then be done by one of two methods: (1) smoking either or both the standard and sphere until their reflectances are exactly equal, or; (2) substituting the ratio of their reflectances into a ponderous algebraic expression. The former method is recommended and was used in this study.

CONTENTS

CONTENTS (cont'd)

EXPLANATION OF SYMBOLS

R = radius of the MgO coated sphere

S = $4\pi R^2$ = total sphere area

a = spherical area of the entrance port

b = spherical area of the exit port

C_e = $a + b$

C = $C_s = C_{st}$ = spherical area of sample and standard ports

C' = $C'_s = C'_{st}$ = plane area of ports C_s and C_{st}

x = $S-a-b-C = S-C-C_e$

r = reflectance of MgO coated sphere wall

r_s = reflectance of sample (or, spherical cap, C_s)

r_{st} = reflectance of standard (or, spherical cap, C_{st})

P = flux received from the source (flux entering the sphere)

B = radiance of the sphere wall with spherical cap C_s in position ($r_s = r_{st}$)

B_o = radiance of sphere wall with black body at C_s

INTRODUCTION

In many phases of protective coatings research, it is often necessary to obtain an absolute evaluation of the reflectance and transmittance characteristics of various surfaces. A knowledge of these characteristics is of paramount importance in the development of coatings and surfaces for the reflection and absorption of electromagnetic radiation. For example, the control of satellite temperatures by manipulation of solar absorptivity-emissivity ratios depends upon the ability to accurately measure the optical properties of its surfaces. The need for both highly absorptive and highly reflective surfaces has been established. It is in the development of these surfaces, particularly surfaces having very low solar absorptivities (α's) of the order of 0.05 - 0.10, that slight errors in the reflectance measurements will cause significant errors in the theoretical calculation of orbital temperatures.

Early work[1, 2] described the case of perfect spheres and, for the most part, neglected the consideration of apertures of a finite size. Taylor[3] discussed the use of absolute methods in which he described a partial integrating sphere. He first determined the average absolute reflectance of the sphere including a flat test plate coated with the sphere coating, which he assumed to have a reflectance identical to that of the sphere wall. He then used the sphere as a substitution instrument by projecting the light source upon the flat plate and obtaining a brightness reading of the sphere wall. He next replaced the standard test plate with an unknown sample plate of different reflectance, and from the ratio of the two wall brightnesses obtained, he concluded the reflectance of the unknown. Like other early workers, he did not consider the effect of the entrance and exit apertures.

Preston[4] applied a more rigorous analysis for the absolute case, and Middleton and Sanders[5] used a still more rigorous theory, using spherical caps rather than flat plates. Neither, however, were able to show that the coating on the test plate had the same reflectance as that of the sphere walls. Consequently, they obtained an average reflectance for the sphere which included the test plate. The plate was probably of a different reflectance. Tellex and Waldron[6] described a similar method.

This report describes an instrument for measuring the absolute spectral reflectance of both diffusely reflecting surfaces and specularly reflecting (mirror-like) surfaces. The integrating sphere reflectometer described is based upon the ability either to insure that the standard possesses a reflectance identical to the sphere coating, or to determine

the value of one in terms of the other. It may be used both as a comparison reflectometer (which approximates an absolute method if the absolute spectral reflectance of the standard is known) and as an absolute reflectometer by use of an involved procedure and a rigorous mathematical analysis.

THEORY OF THE INTEGRATING SPHERE

The theory of the integrating sphere is one of the analysis of multiple reflections in a cavity, requiring the formulation of an integral equation for the inter-reflections. Recently, Jacquez and Kuppenheim[7] have extended the general theory to include five special cases. They considered two types of sphere: (1) the "substitution" type where the standard and sample are alternately placed at the sample aperture and respective measurements made, and (2) the "comparison" type where both the standard and sample are at all times a part of the sphere wall.

For the general case(1) and four special cases, the authors [7] assumed the flux incident upon the entrance and exit apertures to be completely lost to the sphere. Following are the results of their analyses of the special cases.

PERFECT SPHERE

(Standard and sample caps shaped to complete the sphere - See Figures 1 and 2)

Substitution Method

In this case, the sphere contains three ports: an entrance port where the incident light is projected upon the sample, an exit port where the detector views the sphere wall, and a larger sample port. First the standard and then the sample are placed at the sample port, and their respective luminance measured.

The total flux passing through the exit port (to the detector) when the sample is in place is

$$B_S = P r_s \frac{b/S}{1 - (rx/S) - (r_S C/S)} \quad . \qquad . \qquad . \qquad . \qquad . \qquad . \qquad . \qquad . \quad 1$$

(1) The rigorous analysis of the following cases will not be given; see Ref. (7).

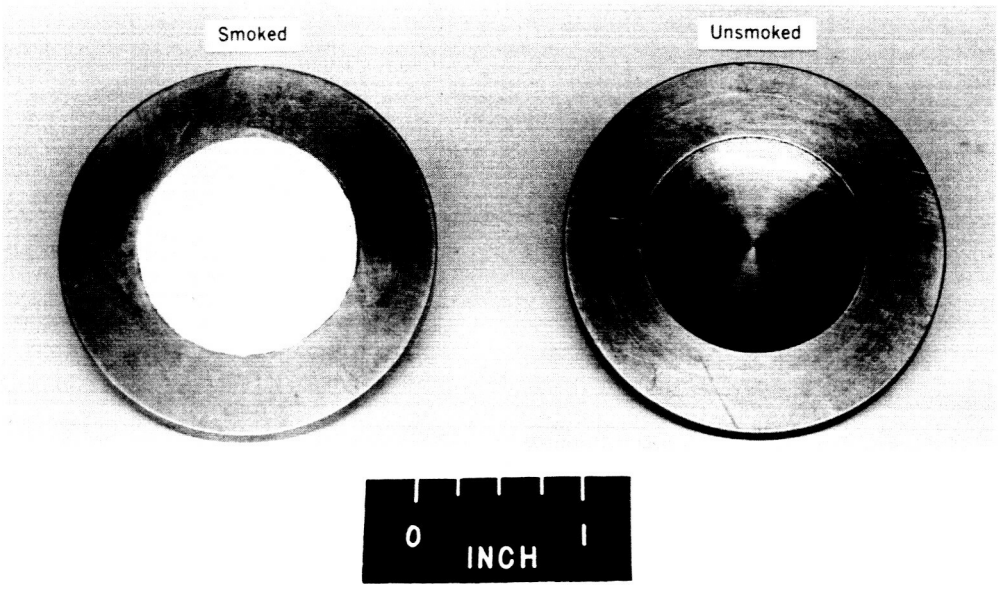

Fig 1 SPHERICAL CAP STANARD

When the standard is substituted for the sample, B_{st} and r_{st} are substituted for B_s and r_s, respectively. Then

$$\frac{B_s}{B_{st}} = \frac{r_s}{r_{st}} \left[1 - \left(\frac{C/S(r_{st} - r_s)}{1 - (rx/S) - (r_s C/S)} \right) \right] ; \qquad \ldots\ldots\ldots\ldots 2$$

The term

$$\frac{b/S}{1 - (rx/S) - (r_s C/S)} \qquad \ldots\ldots\ldots\ldots 3$$

in Equation 1 may be considered the sphere efficiency e, and the term

$$- \frac{C/S(r_{st} - r_s)}{1 - (rx/S) - (r_s C/S)} \qquad \ldots\ldots\ldots\ldots 4$$

in Equation 2 may be considered the error α. It can be seen that the error arises from the different sphere efficiencies when first the standard and then the sample are in place.

Comparison Method

Using this method, both the standard and the sample are in place at all times. In this case, the total flux when the sample is illuminated is

$$B_s = Pr_s \frac{b/S}{1 - (rx/S) - (r_sC/S) - (r_{st}C/S)} ; \quad \ldots\ldots\ldots\ldots 5$$

and the term

$$\frac{b/S}{1 - (rx/S) - (r_sC/S) - (r_{st}C/S)} \quad \ldots\ldots\ldots\ldots 6$$

is the sphere efficiency. Substituting B_{st} and r_{st} for B_s and r_s in Equation 5, the relationship becomes

$$\frac{B_s}{B_{st}} \cong \frac{r_s}{r_{st}} . \quad \ldots\ldots\ldots\ldots 7$$

Thus, the efficiency of the sphere is unchanged whether the sample or standard is illuminated, and the error is zero.

SPHERE WITH FLAT SAMPLE AND STANDARD

Here the analysis becomes more complicated due to non-sphericity of the sample and standard, and to the fact that the sample and standard cannot reflect upon themselves. Hence, only the error terms will be given for the substitution method, the efficiencies being of the same order of magnitude as for the case of the perfect sphere. The error term for the substitution method is given by

$$a \cong - \frac{(r_{st} - r_s)(C/S)(rx/S)}{1 - (rx/S) - (r_sC/S)(rx/S)} . \quad \ldots\ldots\ldots\ldots 8$$

In the comparison method, the efficiency is given by

$$e \cong C/S(2r - r_s - r_{st}); \quad \ldots\ldots\ldots\ldots 9$$

and the error term is

$$a \cong \frac{C/S(r_{st} - r_s)}{1 - (r_sC/S)} . \quad \ldots\ldots\ldots\ldots 10$$

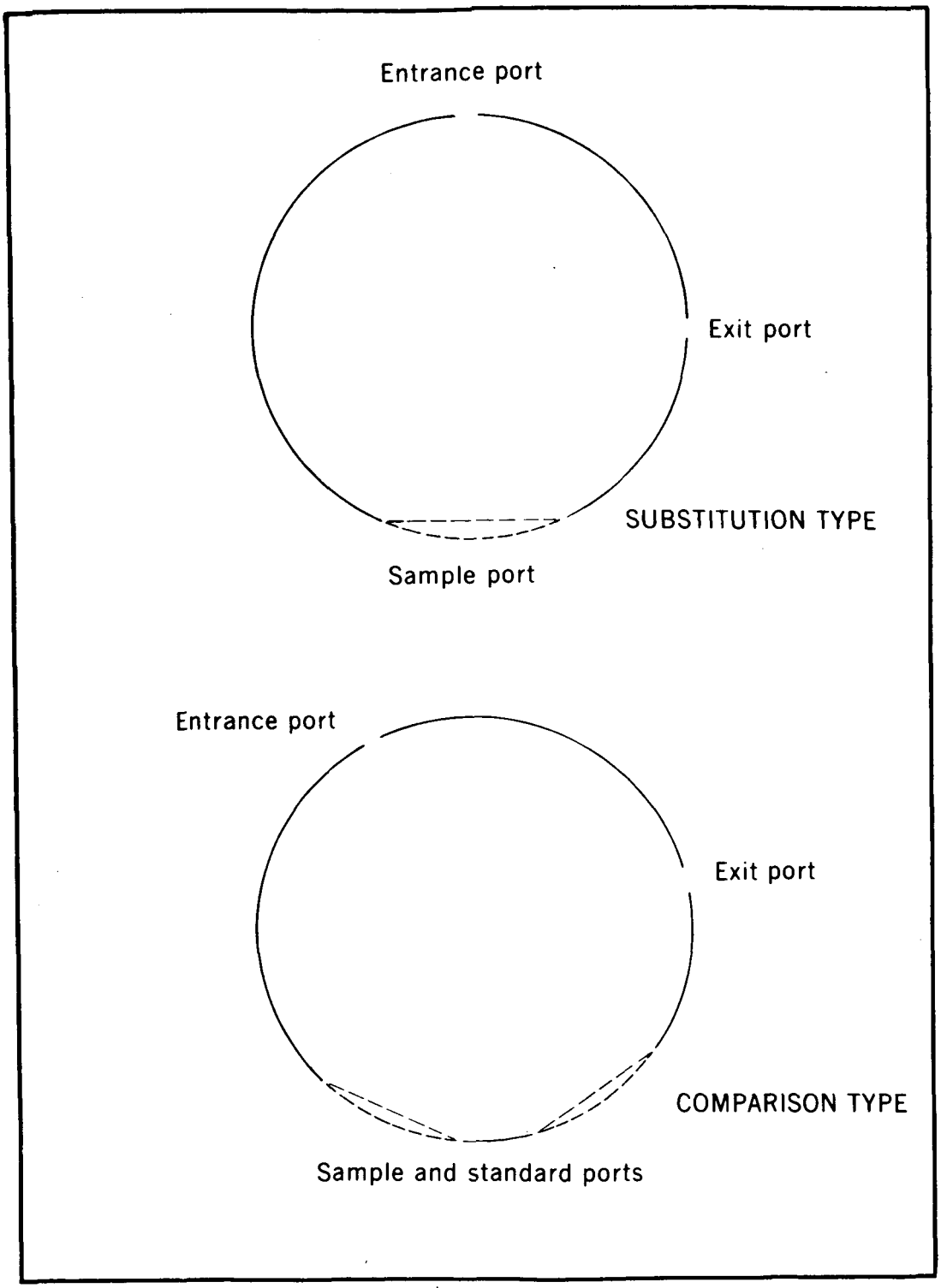

Fig. 2 TWO TYPES OF INTEGRATING SPHERES

Jacquez and Kuppenheim obtained the following differentials;

$$\frac{\partial e}{\partial r} > 0, \qquad \frac{\partial e}{\partial (b/S)} > 0, \qquad \frac{\partial e}{\partial (a/S)} > 0,$$

and $\frac{\partial e}{\partial (C/S)} < 0$ provided $(2r - r_s - r_{st}) > 0$; showing that for a given sphere radius, maximum sphere efficiency is obtained when r and b/S are as large as possible and a/S and C/S as small as possible. The limiting factor for the size of the exit port b will be the size of the entrance aperture to the monochromator. Therefore, in general, $B_{st} = P r_{st} e_{st}$ and $B_s = P r_s e_s$ for the substitution method. For the comparison method for flat samples,

$$\frac{B_s}{B_{st}} = \frac{r_s e_s}{r_{st} e_{st}} ;$$

and for the comparison method with spherical sample and standard,

$$\frac{B_s}{B_{st}} = \frac{r_s}{r_{st}} .$$

THE REFLECTOMETER DESIGN

From the foregoing, it may be seen that the choice of geometry is arbitrary within certain limits, and that the sphere efficiency, e, and the error, α, decrease with increasing sphere diameter. Thus, in order to minimize the error (for flat samples), a relatively large sphere diameter of eight inches was chosen at some expense of efficiency.

The general sphere design is given in Figure 3 where a, b, C_s, and C_{st} are the entrance, exit (photocell), sample and standard apertures respectively. The sphere rests upon spindles equipped with adjustable stops. The entrance and exit ports are each 55°36' from the axis, and are offset 6°30' to the normal such that the angle of incidence to the sample at position C_2 and to the normal at "i" is approximately 7°. The sphere can be turned through exactly 180°; thus, the function of the apertures a and b are interchangeable and the samples can first be illuminated and the wall viewed, and conversely, the wall illuminated and the samples viewed, (see Figure 4). The initial illumination and projection on the sphere wall of the reflected specular component (first reflection) are shown in Figure 5. By use of a screen with circular aperture, h, the illuminated spot, i, on the wall may or may not be included in the flux entering the monochromator-detector system.

The sphere was machined in two flanged hemispheres from 6061-T6 aluminum stock and provided with a high polish(1). The method used in coating the sphere is that of the National Bureau of Standards and consists of burning Grignard Reagent-Grade magnesium turnings raked into a cone. The instructions[8] issued by the Bureau were followed as closely as possible in coating the sphere. The dimensions of the sphere are given in Table I.

The optical system is built around the Perkin-Elmer 112U Spectrophotometer. This instrument utilizes a Model 99 double pass-single beam monochromator and a universal source assembly. The source assembly contains placements for a globar, which is heated to 1100°C by about 200 watts input, as an infrared source, and a tungsten strip filament lamp for a visible light source. This tungsten strip filament lamp has its greatest output in the range of 0.37 to 2 microns. In order to focus either infrared or visible radiation on the entrance port of the sphere, the assembly uses front surface aluminized mirrors which are free from chromatic aberration.

Table I

SPHERE CONSTANTS

Dimension	Symbols	Values
Sphere radius, inches	R	3.985
Total surface area	S	199.55726
Radius of exit port		0.2467
Radius of sample ports		0.6900
Spherical area of exit plus source ports	C_e	0.38339
Spherical area of the sample ports	C	1.50682
$S - C - C_e$	x	197.66705

(1) A 1.5 - 2mm layer of freshly smoked MgO on a polished aluminum surface approximates an infinitely thick layer of MgO.

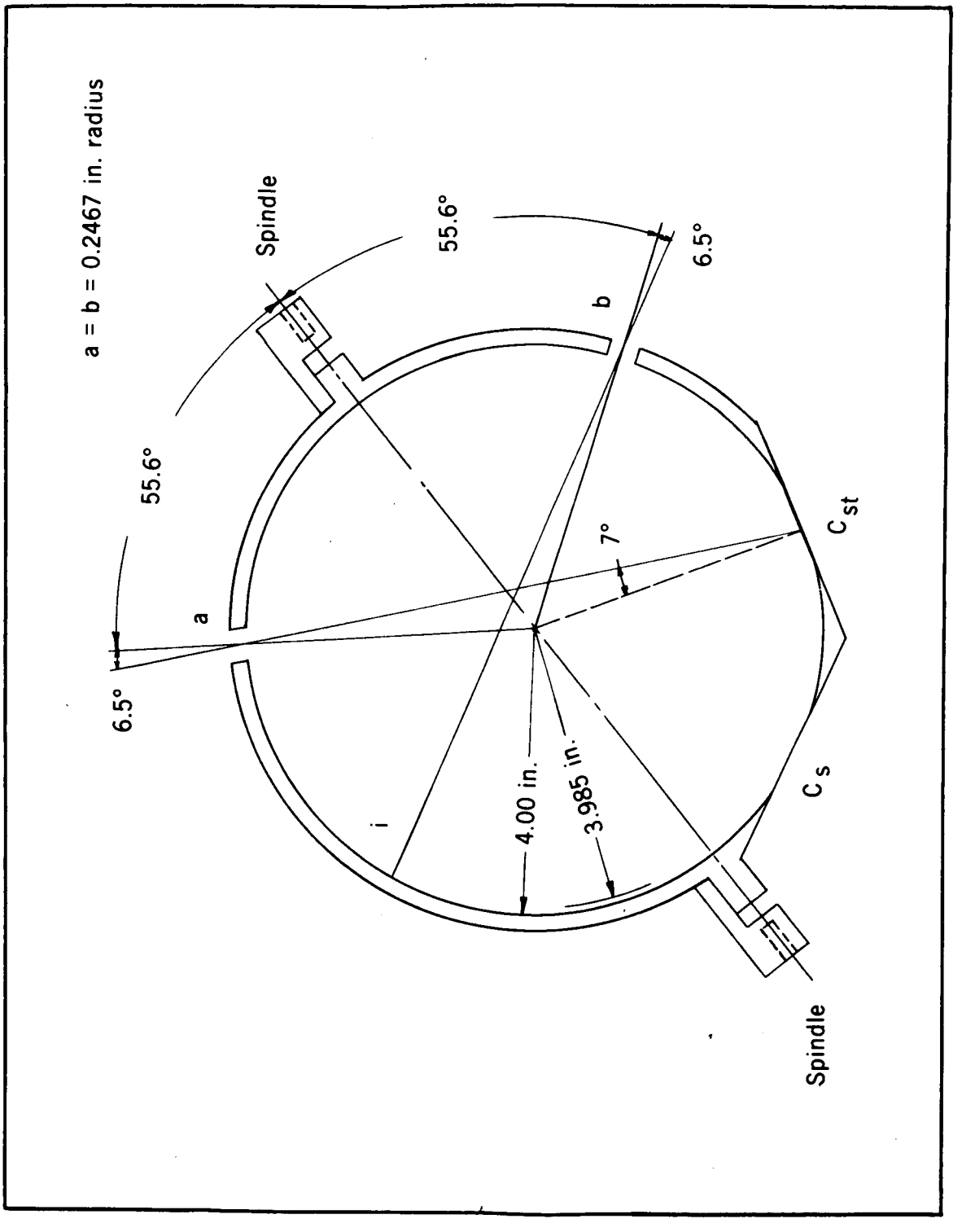

Fig. 3 GENERAL SPHERE DESIGN

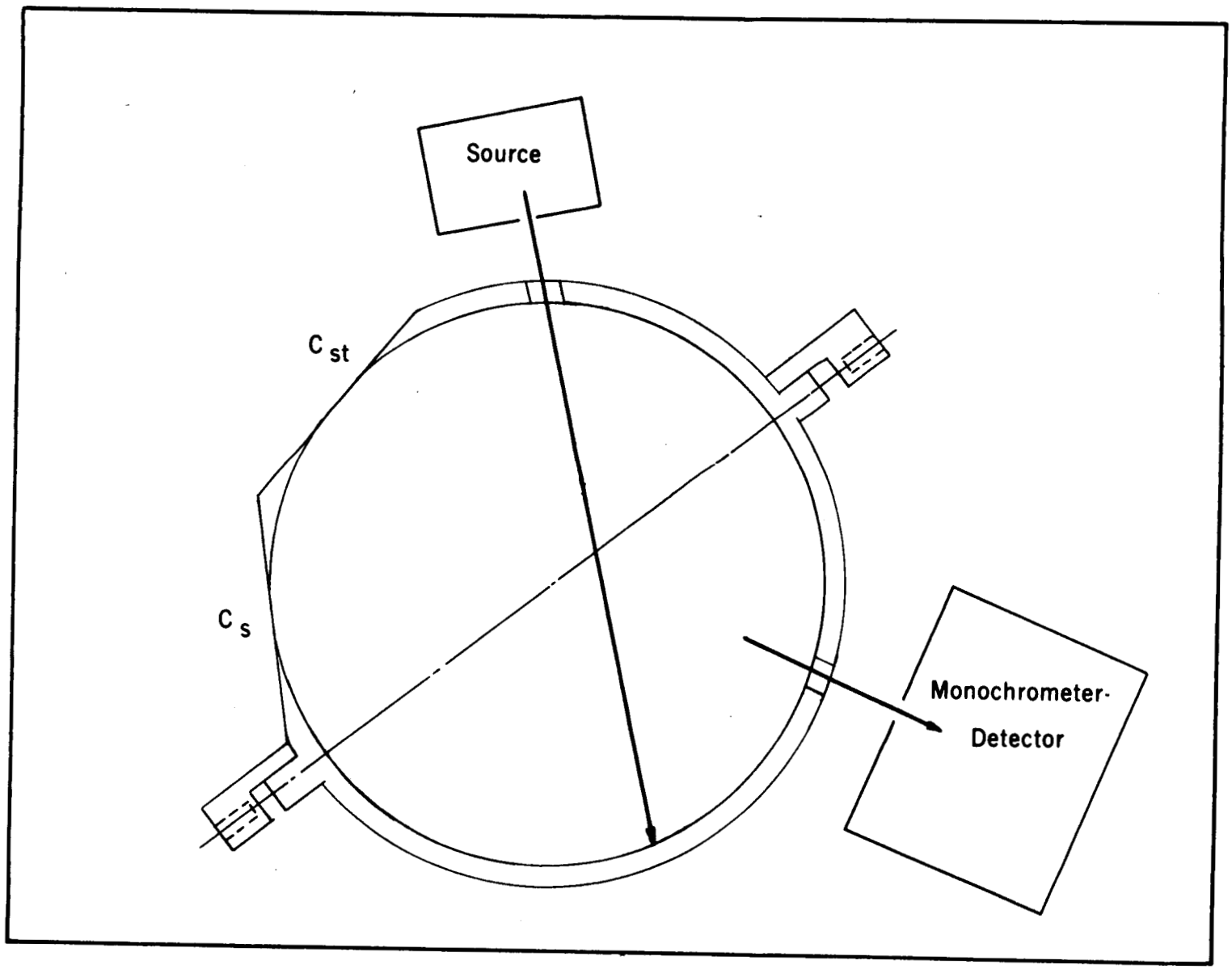

Fig. 4 SPHERE POSITION REVERSED

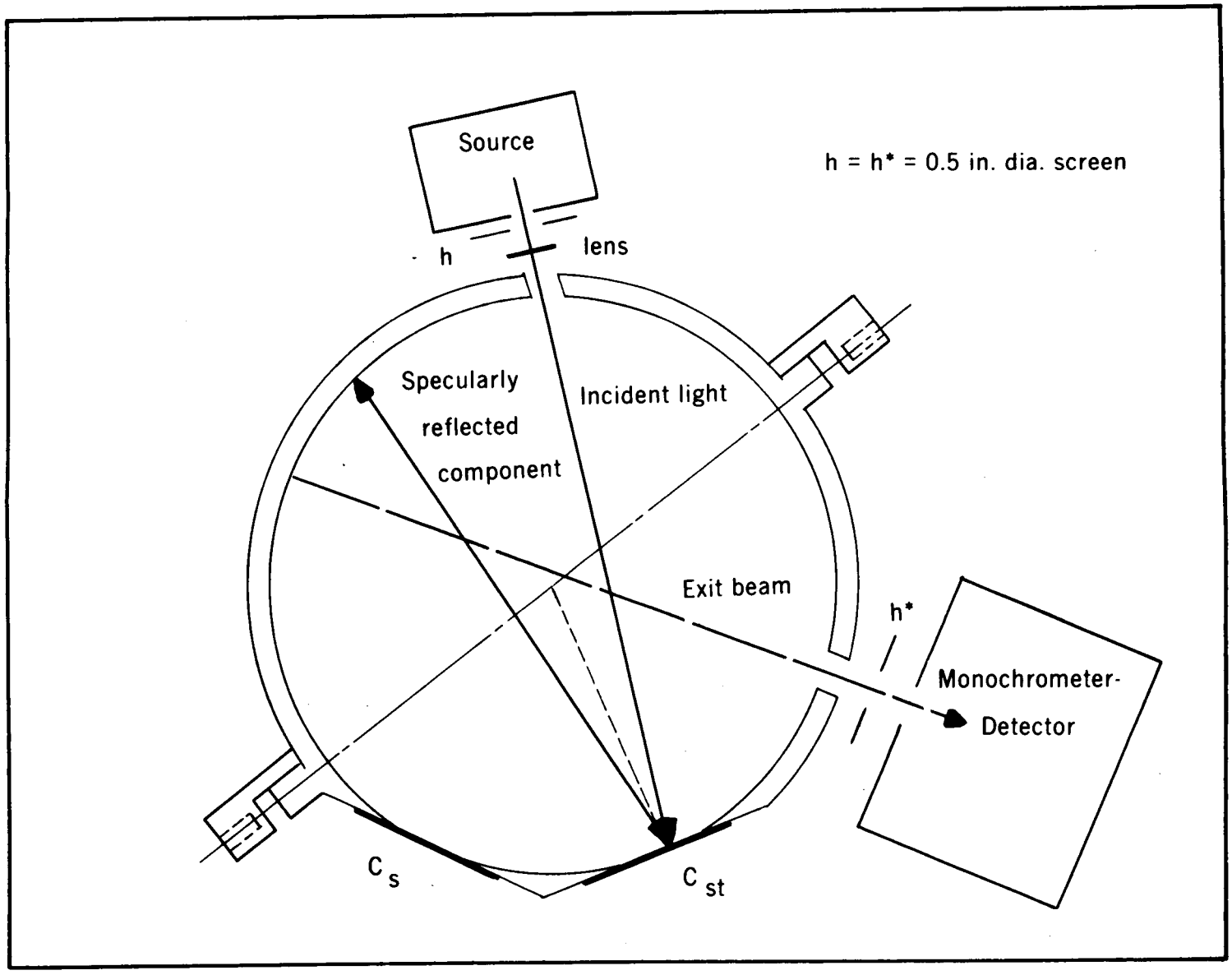

Fig. 5 RELATION OF SPHERE TO COMPONENTS

For the measurement of absolute hemispherical spectral reflectance between 0.37 and 2.5 microns, the source assembly is placed such that the incident light is slightly off perpendicular to the sample. The light coming from either the tungsten unit or globar is collected on a flat, front-surfaced mirror, which, in turn, directs it to a spherical focusing mirror. Between the spherical mirror and the sphere entrance port, there is a 1/2 inch restricting aperature that shields the sphere and monochromator from secondary reflections. A spherical quartz lens with a four inch focal length is placed between the restricting aperature and the sphere entrance port in order to focus the light so that it nearly fills the sample port. Care was taken to insure that the light beam on the sample port did not fall over onto the sphere wall. The entire arrangement is such that the primary reflection from the sample does not fall back on the incident beam, but slightly to the side at an angle of approximately 14°. This prevents the monochromator from picking up any directly reflected light from the sample. Multiple reflections within the sphere present a diffuse light source to the monochromator optics.

For ultraviolet reflectance measurements, a 5,000 volt hydrogen arc point source is beamed directly into the sphere with the 1/2 inch restricting aperature and the quartz lens for focusing. The light path in the sphere is the same as for visible and infrared reflectance measurements. The diffuse light beam from the sphere passes through a 2mm entrance slit and is collimated by an off-axis paraboloid mirror and then refracted by the prism. A "Littrow" mirror returns the radiation which is refracted by the prism. The energy is focused by the paraboloid mirror in a dispersed field in the vicinity of the entrance slit. A portion of this field is intercepted by an aluminized front surfaced flat mirror. This, in turn, is brought to focus between the halves of the split mirror. The energy is modulated and slightly displaced by a 13 cycle per second chopper and returned for a second pass through the paraboloid-prism-Littrow system, where it receives a second dispersion. After the second pass, the beam is reflected by another front surfaced mirror and brought to focus in a spectrum falling across the exit slit. The exit slit permits only chopped radiation of a narrow wavelength band, whose band width is a function of the slit opening, through to the detector system. Figure 6 presents a graphic outline of the entire optical system

Three detectors are used in the range 0.2 to 2.5 microns wavelength. From 0.2 to 0.75 microns, a 1P28 photomultiplier is used; from 0.75 to 0.90 microns wavelength, a 1P21 is used; from 0.90 to 2.5 microns, a lead-sulfide detector is utilized. The use of this type of detector system permits a maximum sensitivity for each small wavelength region. The detector signals are picked up by a 13 cycles per

second amplifier and rectified by breaker type synchronous rectifiers that are actuated by the rotation of the chopper shaft. Noise components are removed by electrical filters in the amplifier unit.

ANALYSIS OF THE SPHERE WHEN USED AS AN ABSOLUTE REFLECTOMETER

To conduct a mathematical analysis of the designed system when determining absolute reflectance, the conditions shown in Figure 5 were considered. That is, the entering flux is incident upon the spherical cap at C_{st} and the monochromator-detector system views the sphere wall. The reflectance of the two spherical caps is made equal, so that $r_s = r_{st}$. This is accomplished by smoking the caps with MgO until no change in the radiance, B, of the sphere wall is noted when the sphere is used as a comparison instrument as discussed previously.

With a black body in position at C_s, the first reflected flux escaping from the sphere is equal to the product of the first reflected flux, $r_s P$, and the ratio of the area of the ports to that of the complete sphere. Therefore, assuming the sphere surface to be Lambertian,

$$P_1 = r_s P \frac{(C + C_e)}{S} \quad . \qquad \ldots\ldots\ldots 11$$

We next derive a lemma, proven by Preston[4], concerning the multiple reflected flux escaping from the sphere. For a sphere having a total spherical area S, a uniform wall radiance B and two apertures with plane areas Y and Z cutting off spherical areas Y_s and Z_s, the multiple reflected flux escaping from the sphere is:

Flux escaping = Flux that would go to Y if the sphere were complete
+ the flux that would go to Z if the sphere were complete
- the flux that would go out Y originating from the spherical cap Z_s
- the flux that would go out Z originating from the spherical cap Y_s

$$= \pi BY + \pi BZ - \pi BY_sZ_s/S - \pi BZ_sY_s/S$$
$$= \pi B \frac{(Y + Z - 2\,Y_sZ_s)}{S}$$

Thus, the multiple reflected flux escaping from the sphere is

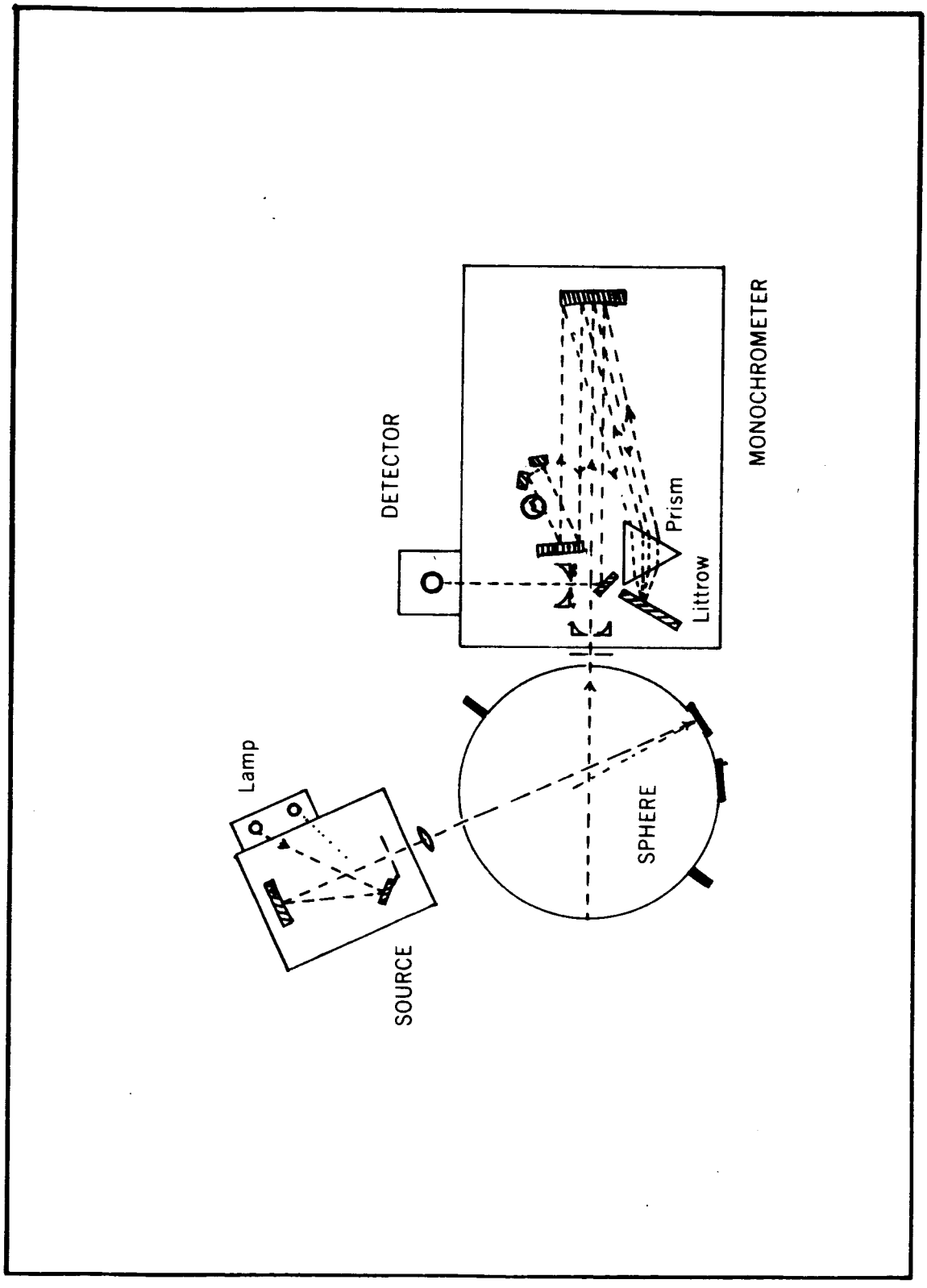

Fig. 6 THE OPTICAL PATH

$$P_2 = \pi B_o(C' + C_e - \frac{2CC_e}{S}) \quad ; \qquad \ldots\ldots\ldots\ldots 12$$

where C_e is taken as both the spherical and plane areas of the entrance and exit ports. The total flux received by the rest of the sphere is, then

$$P' = P + \pi B_o \left[\left(\frac{x - C}{r}\right) + \frac{C}{r_s}\right] \quad . \qquad \ldots\ldots\ldots\ldots 13$$

Therefore, the amount absorbed in the surface is

$$P_3 = \left[(1 - r)\left(\frac{x - C}{x}\right) + (1 - r_s)\frac{C}{x}\right] P' \quad ;$$

and substituting for P', we obtain

$$P_3 = \left[(1 - r)\left(\frac{x - C}{x}\right) + (1 - r_s)\frac{C}{x}\right]\left[P + \pi B_o\left(\frac{x - C}{r}\right) + \frac{\pi B_o C}{r_s}\right] \quad , \qquad \ldots\ldots\ldots\ldots 14$$

Therefore, the total flux may be equated as follows:

$$P = P_1 + P_2 + P_3. \qquad \ldots\ldots\ldots\ldots 15$$

By substituting Equations 11, 12, and 14 in Equation 15, we obtain

$$P = r_s P\left(\frac{C + C_e}{S}\right) + \pi B_o(C' + C_e - \frac{2CC_e}{S}) + \left[(1 - r)\left(\frac{x - C}{x}\right) + (1 - r_s)\frac{C}{x}\right]\left[P + \pi B_o\left(\frac{x - C}{r}\right) + \frac{\pi B_o C}{r_s}\right] \quad . \qquad \ldots\ldots\ldots\ldots 16$$

Solving for $\pi B_o/P$, we obtain

$$\frac{\pi B_o}{P} = \frac{1 - r_s(C + C_e)/S - (1 - r)(x - C)/x - (1 - r_s)C/x}{C' + C_e - \frac{2CC_e}{S} + \left[\left(\frac{x - C}{r}\right) + \frac{C}{r_s}\right]\left[(1 - r)\left(\frac{x - C}{x}\right) + (1 - r_s)\frac{C}{x}\right]} \quad . \qquad \ldots\ldots\ldots\ldots 17$$

Next, the black body is removed from the aperture C_s and a spherical cap having a reflectance $r_s = r_{st} \neq r$ is placed over the aperture C_s to complete the sphere, except for the entrance and exit ports. The analysis for this case is similar to the case for the black body at C_s. The first reflected flux escaping from the sphere is

$$P_1 = r_s P C_e / S \; ; \qquad \ldots\ldots\ldots\ldots 18$$

and the multiple reflected flux escaping is

$$P_2 = \pi B (a + b - \frac{2ab}{S}).$$

But $a = b = C_e/2$; therefore,

$$P_2 = \pi B (C_e - \frac{C_e^2}{2S}) \; , \qquad \ldots\ldots\ldots\ldots 19$$

Since the dimension C_e is much smaller than S, the term $C_e^2/2S$ may be neglected, and the multiple reflected flux escaping from the sphere is simply,

$$P_2 \approx \pi B C_e . \qquad \ldots\ldots\ldots\ldots 20$$

The flux received by the remainder of the sphere (including the spherical caps C_s and C_{st}) is

$$P'' = P + \pi B \left[\left(\frac{x - C_2}{r} \right) + \frac{C_1}{r_1} + \frac{C_2}{r_2} \right] .$$

But, $C_s = C_{st} = C$ and $r_s = r_{st}$; therefore,

$$P'' = P + \pi B \left[\left(\frac{x - C}{r} \right) + \frac{2C}{r_s} \right] . \qquad \ldots\ldots\ldots\ldots 21$$

For simplicity, we will let $S - C_e = d = x + C$. Then, the amount of flux absorbed in the surface is

$$P_3 = \left[(1 - r) \left(\frac{d - C_1 - C_2}{d} \right) + (1 - r_1) \frac{C_1}{d} + (1 - r_2) \frac{C_2}{d} \right] P''$$

However, $C_s = C_{st} = C$ and $r_s = r_{st}$. Therefore,

$$P_3 = \left[(1 - r) \left(\frac{d - 2C}{d} \right) + 2(1 - r_s) \frac{C}{d} \right] P''. \qquad \ldots\ldots\ldots\ldots 22$$

Substituting Equation 21 in Equation 22, we obtain for the total flux absorbed

$$P_3 = \left[(1 - r)\left(\frac{d - 2C}{d}\right) + 2(1 - r_s)\frac{C}{d}\right]\left[P + \pi B\left\{\left(\frac{x - C}{r}\right) + \frac{2C}{r_s}\right\}\right] . \quad \ldots\ldots\ldots 23$$

We next equate the total flux

$$P = P_1 + P_2 + P_3. \quad \ldots\ldots\ldots 24$$

Substituting Equations 18, 20, and 23 in Equation 24, we obtain

$$P = r_s P\frac{C_e}{S} + \pi B C_e + \left[(1 - r)\left(\frac{d - 2C}{d}\right) + 2(1 - r_s)\frac{C}{d}\right]\left[P + \pi B\left\{\left(\frac{x - C}{r}\right) + \frac{2C}{r_s}\right\}\right] . \quad \ldots\ldots\ldots 25$$

Solving for $\pi B/P$, we obtain

$$\frac{\pi B}{P} = \frac{1 - r_s C_e/S - (1 - r)(d - 2C)/d - (1 - r_s)\,2C/d}{C_e + \left[\left(\frac{x - C}{r}\right) + \frac{2C}{r_s}\right]\left[(1 - r)\left(\frac{d - 2C}{d}\right) + \frac{2C(1 - r_s)}{d}\right]} . \quad \ldots\ldots\ldots 26$$

We next divide Equation 17 by Equation 26 and obtain

$$\frac{B_o}{B} = \frac{\left\{1 - \frac{r_s(C + C_e)}{S} - (1 - r)\left(\frac{x - C}{x}\right) - (1 - r_s)\frac{C}{x}\right\}\left\{C_e + \left[\left(\frac{x - C}{r}\right) + \frac{2C}{r_s}\right]\left[(1 - r)\left(\frac{x - C}{d}\right) + \frac{2C(1 - r_s)}{d}\right]\right\}}{\left\{1 - r_s\frac{C_e}{S} - (1 - r)\left(\frac{x - C}{d}\right) - \frac{2C(1 - r_s)}{d}\right\}\left\{\left[C' + C_e - \frac{2CC_e}{S}\right] + \left[\left(\frac{x - C}{r}\right) + \frac{C}{r_s}\right]\left[(1 - r)\left(\frac{x - C}{x}\right) + (1 - r_s)\frac{C}{x}\right]\right\}} . \quad \ldots\ldots\ldots 27$$

Thus, we obtain the absolute reflectance, r_s, of the spherical cap standard, C_s (and C_{st}), by first measuring r in terms of r_s by the comparison technique and then measuring the ratio B_o/B by the absolute method.

We may reduce Equation 27 to a simpler form by insuring that $r = r_s$. Letting $r = r_s$ and remembering that $d = S - C_e = x + C$, Equation 27 reduces to

$$\frac{B_o}{B} = \frac{x}{S - C_e}\left[\frac{(1 - r)(S - C_e) + rC_e}{r(C' + C_e - \frac{2CC_e}{S}) + x(1 - r)}\right], \quad \ldots\ldots\ldots 28$$

which is identical to the expression obtained by Middleton and Sanders[5].

PROCEDURE FOR OBTAINING ABSOLUTE VALUES

When determining the absolute spectral reflectance of a standard, the sphere and spherical caps(1) are given a fresh coat of MgO. The sphere is assembled as shown in Figure 5 with the light incident upon the sample port at C_{st}. The spherical caps (samples) are placed in the sphere. The reflectance of one with respect to the other is measured by the comparison technique (Equations 5, 6, and 7). Their reflectances are made equal, if necessary, by resmoking one or both caps with further increments of MgO until $r_s = r_{st}$ for C_s and C_{st} respectively.

The screen, h, is then replaced by a focusing lens placed adjacent to the exit port, or by a light cone arrangement as was used in this study (see Figure 7). Thus, all the light passing through the port, or a reproducible fraction, is received by the detector. The response of the detector at the exit port will then be proportional to the total flux passing through the port, and is noted as B_{r_s}.

The sphere is then turned 180° upon its axis so that the light will be projected upon the sphere wall and the sample port C_{st} viewed by the monochromator Since the flux B passing through the exit port is a function of the first reflection only in this case (Equation 5), the response of the detector is noted as B_r. Thus, if the spherical caps have the same reflectance as the sphere coating ($r = r_s = r_{st}$), the measured fluxes for both positions will be equal ($B_r = B_{rs}$). If $B_r \neq B_{r_s}$, the reflectances of the spherical caps and the sphere are made equal by resmoking.

The absolute spectral reflectance can then be determined for the sphere; and thus, for the spherical cap standards. This can be accomplished with the sphere in either position(2) and involves obtaining a

(1) With spherical depressions of exactly the same radius as the sphere and exactly the same diameters as the sample ports.

(2) The position shown in Figure 3 with the light incident upon the spherical cap C_{st} was used in this study.

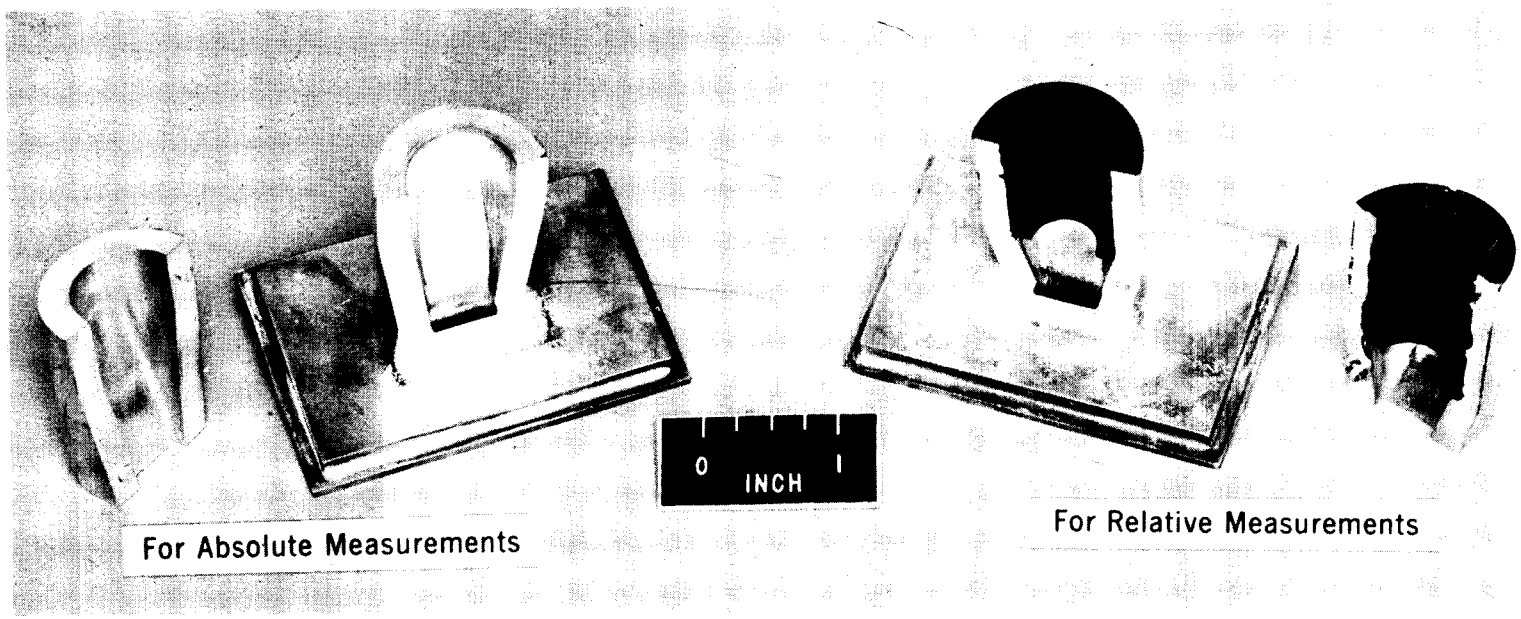

Fig. 7 LIGHT CONES

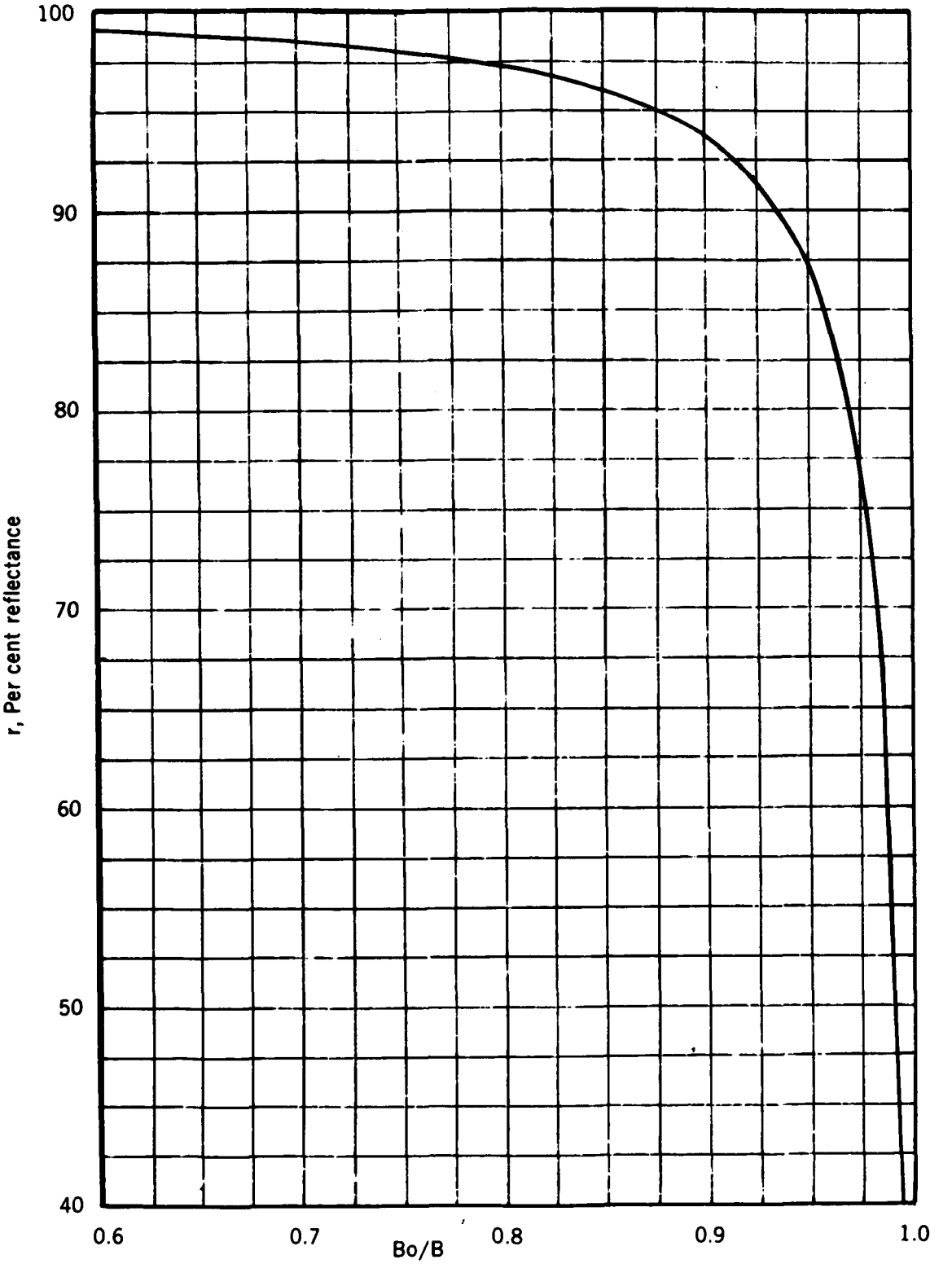

Fig. 8 ABSOLUTE REFLECTANCE FROM EQUATION 28

brightness measurement, B, with both C_s and C_{st} in position, and then the brightness B_o with C_s replaced by a black body(1). The ratio B_o/B may then be used to calculate the absolute reflectance from Equation 28. The values B_o/B may be plotted against absolute reflectance, r, for any given set of sphere dimensions using Equation 28 and the values reported in Table 2. Figure 8 is the plot obtained for the sphere described in this report. The values of absolute reflectance at any wavelength can be read directly from the curve. The spherical cap standard, whose absolute hemispherical spectral reflectance is known, can then be used to measure the reflectance of other surfaces by the comparison technique discussed earlier in this report.

EXPERIMENTAL RESULTS

The absolute hemispherical spectral reflectance of the magnesium oxide smoked spherical cap standard as measured with the instrument described is presented in Curve A, Figures 9 and 10. Curve D, Figure 9, shows the reflectance of a freshly shaved magnesium carbonate block. These values were obtained by comparison to the magnesium oxide standard whose absolute reflectance is known.

The reflectance of paints pigmented with rutile titanium dioxide and red iron oxide are presented in Curves B and C, respectively, Figures 9 and 10. The figures show the values obtained on our instrument and those obtained for the same paints on a MIT-Hardy Recording Spectrophotometer in the 0.4 - 0.7 micron wavelength range, and on a Preston-type sphere in the 1.0 - 2.5 micron wavelength range.

DISCUSSION

The visible reflectance curves obtained with the MIT-Hardy instrument were higher than those determined on our instrument. The higher values are primarily due to the use of a magnesium carbonate standard with an assumed reflectance of 100% on the MIT-Hardy instrument. This can be seen readily from Figure 9, where it will be noted that a freshly scraped $MgCO_3$ block has an average reflectance of 95%, when compared to our MgO standard at an average of 97.5% absolute reflectance in the visible region of the spectrum.

(1) A completely darkened room approximates a black body in the wavelength region studied.

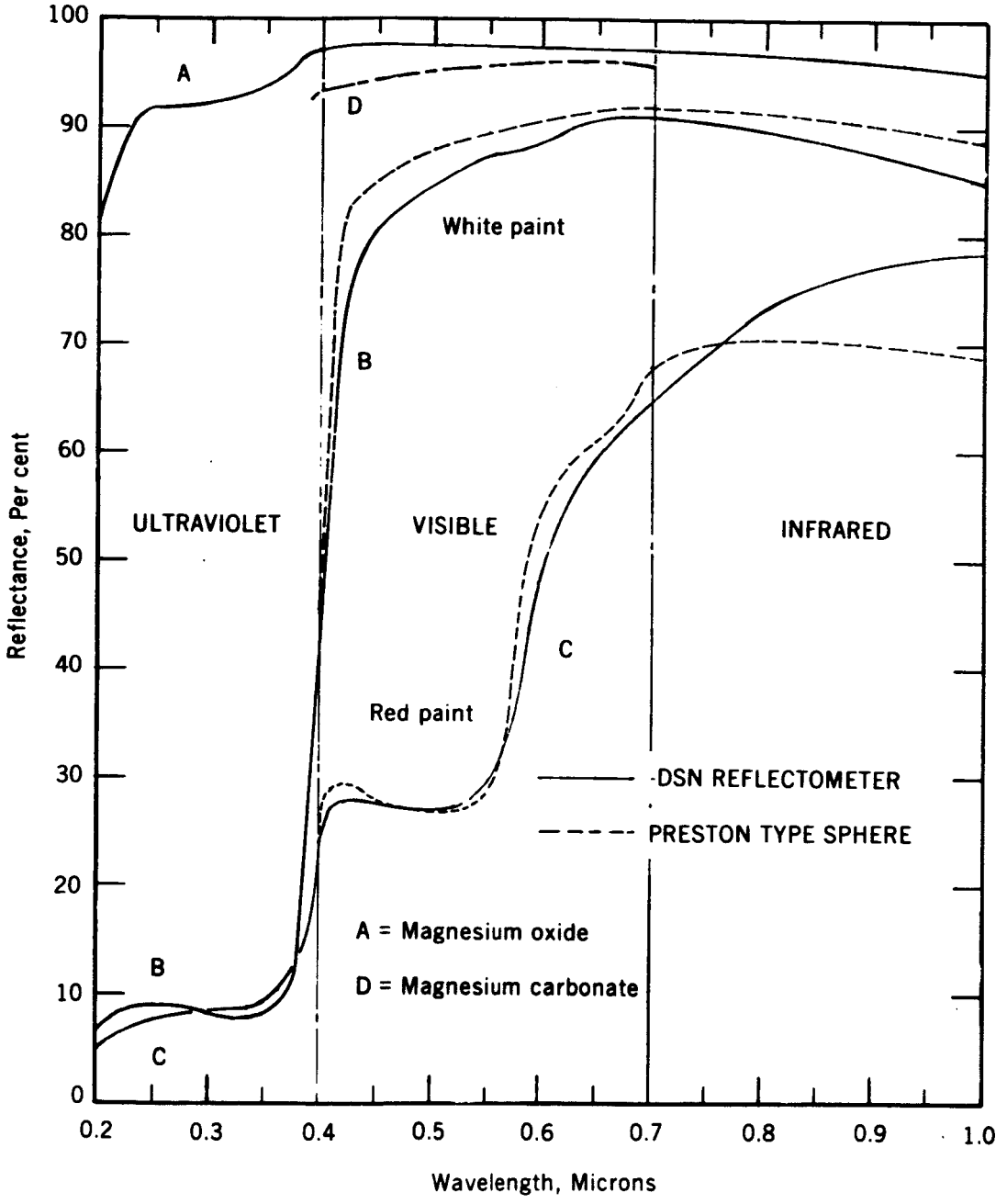

Fig. 9 ULTRAVIOLET AND VISIBLE REFLECTANCE OF SEVERAL MATERIALS

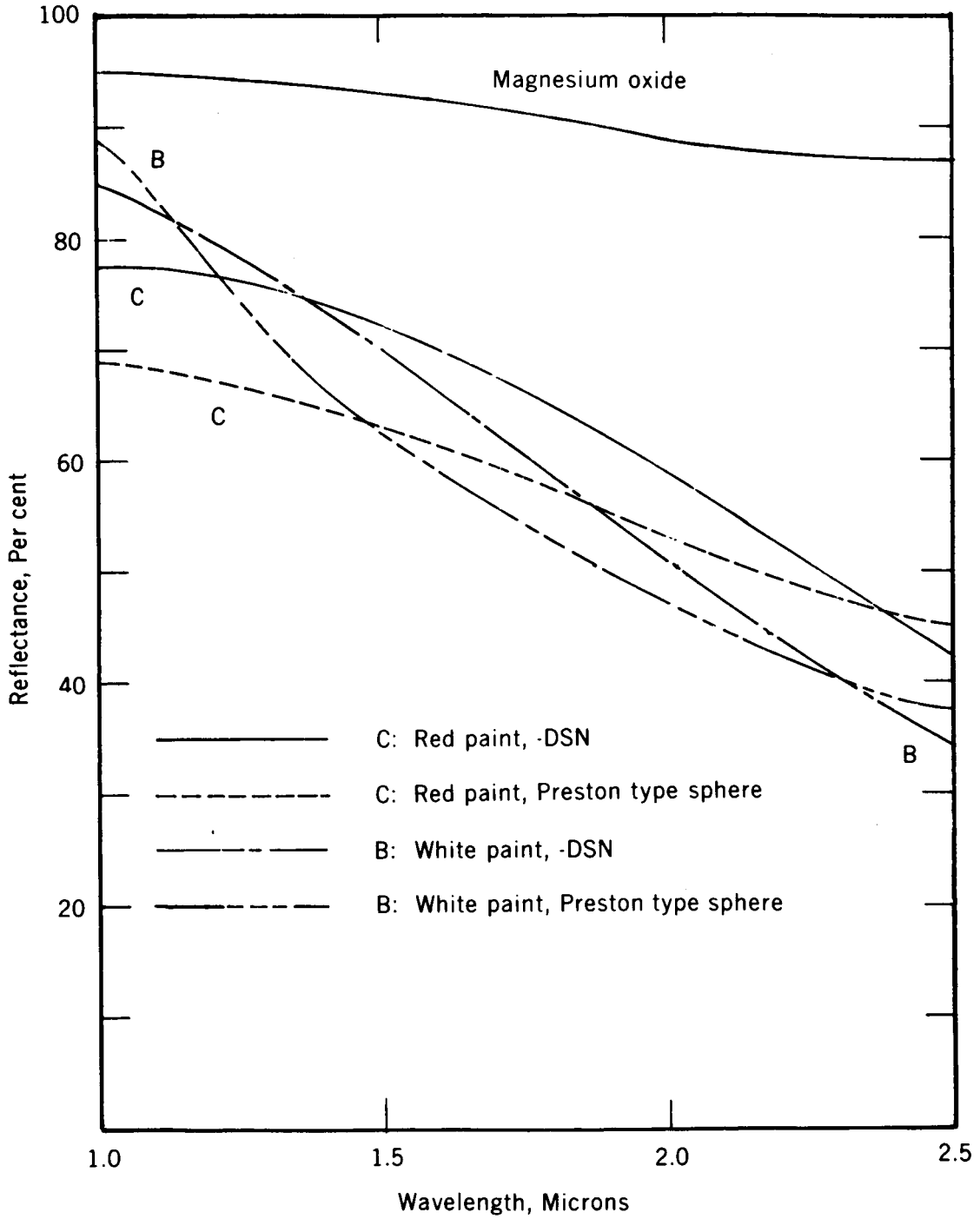

Fig. 10 INFRARED REFLECTANCE OF SEVERAL MATERIALS

It should be noted that our curve does not represent the absolute reflectance of magnesium oxide per se, but rather it represents the absolute reflectance of the particular magnesium oxide standard which we prepared. The reflectance of magnesium oxide is dependent upon thickness, the nature of the substrata, its age and the technique of deposition. However, the curves for MgO presented in Figures 9 and 10 agree closely with the values reported by other workers[9, 10] and our values are somewhat lower than the values reported by Betz et al[9] beyond 1.5 microns wavelength.

It is in the infrared that our results differ most significantly from the values obtained on the Preston sphere for the same materials (Curves B and C, Figures 9 and 10). At first thought, one might suspect an error in our values due to an error in measuring the absolute reflectance of the magnesium oxide standard to which we compared the two paints. However, since the absolute reflectance of our standard is slightly lower in the infrared than that reported by others for like thicknesses, any error would be expected to be negative when comparing other surfaces to it.

We have shown in Appendix I that the theoretical error in our measurements of the absolute reflectance of the standard (thus, the sphere wall) does not exceed $\pm$ 0.1%, and approaches zero beyond 1.5 microns wavelength (below 93% reflectance). Similarly, we have shown that the theoretical error in comparing other surfaces to magnesium oxide, although positive, does not exceed 0.3%. However, this does not account for the differences in the results of our measurements and those obtained on a Preston-type sphere.

The analyses in Appendices II and III appear to account for these differences. The absolute reflectometers reported in the literature to-date have not been provided with a means for insuring that the test plate has a reflectance identical to that of the sphere wall. We have found on numerous occasions that this may exceed 5% differences for aged sphere coatings. Furthermore, the type and condition of the substrata affects the reflectance changes due to aging. Thus, since we have insured that the reflectances of the test plate (spherical cap standard) and sphere wall differed by no more than $\pm$ 0.1% in the entire 0.2 - 2.5 micron wavelength range, we were able to minimize the errors. This was accomplished by smoking either or both the sphere wall and spherical cap until $r_s = (1.000 \pm 0.001) r$ for the particular wavelength range in which we were working, as discussed previously. The aluminum sphere was provided with a higher polish than the spherical caps. Thus, it was necessary to smoke the cap with further increments of magnesium oxide as we worked at longer and longer wavelengths.

Most integrating spheres reported in the literature have the detector mounted to the exit port; and for instruments employed in measuring spectral values, the sphere receives only monochromatic light, where the monochromator is placed between the source and the sphere. In our method, the monochrometer is placed between the sphere and the detector, providing some advantages as well as disadvantages over the other method (Figures 6).

The advantages of our arrangement are:

(1) Most detectors are angularly selective; thus, the angular characteristics of the sample and standard will not affect the detector by our method, since the light passes through the monochromator before impinging upon the detector.

(2) Gray body emission of the sample and sphere, due to the heating effect when working in the infrared, will have less effect than when the detector is mounted on the sphere wall. This is due to the fact that a sphere-wall-mounted detector will receive all radiation coming from the sphere and sample, i.e., both reflected and emitted energy.

(3) Anisotropic samples, when rotated in polarized light, reflect such light differently. Since the light from a monochromator is more or less polarized, depending upon the optical system of the specific instrument, this error is eliminated in our instrument where the light entering the sphere is polychromatic.

(4) When the detector is mounted away from the sphere, rough or grained surfaces which reflect more energy is one direction than in another will not cause the degree of error that might occur if the detector is mounted on the sphere wall.

The disadvantages are:

(1) Considerable intensity is lost when the light beam is passed through the monochromator before reaching the detector. This limits the long wave usefulness of the instrument for any given source and necessitates driving the amplifier to a point which results in a high noise level.

(2) The impingement of the polychromatic beam upon the sphere and sample tends to cause some heating due to absorption, particularly for dark samples and when working in the infrared.

(3) The use of a polychromatic entering beam tends to discolor the sphere coating when working in the ultraviolet with the continuous hydrogen arc source. This necessitates making the ultraviolet measurements last in a given series, and recoating the sphere before each series is made.

CONCLUSIONS

The reflectometer described in this report may be used to determine accurately the absolute hemispherical spectral reflectance of most surfaces. It may be used as a comparison instrument to obtain values approaching absolute by first determining the absolute reflectance of the standard and sphere wall. It is in this respect that the instrument is unique; that is, the absolute values of the magnesium oxide standard may easily be monitored at any time during the course of comparison measurements.

FUTURE PROGRAMS

The three major problems that have evolved during the course of this work are: 1) the low energy input to the monochromator-detector system, 2) the lack of a highly reflective, diffuse sphere coating for use at wavelengths beyond 3 microns, and 3) the manual operation of the instrumentation which is tedious and time consuming.

There are several possibilities to correct the low energy output from the radiation sources now employed. One method is the use of present sources, or a new, more intense source, with a better collecting system for delivery to the sphere. Other possibilities are the use of such sources as a free burning D. C. arc, a constricted arc, or a low order plasma jet either in air or in vacuum. Thus, color temperatures on the order of 6000°K (solar) to 30,000°K are possible. These are considerably above the temperature of sources now used. Any of the above sources will produce a continuous spectrum, thus simplifying our source system. An optical focusing system can be easily designed around any of the above sources.

With an increase in the intensity of the light delivered to the sphere, a slit-servo programming system operated by electrical cams for a given spectral region may be used. Such a modification will make the reflectometer virtually automatic.

The problem of a diffuse, highly reflecting sphere coating for use in the infrared beyond 3 microns wavelength is one which will be more difficult to solve. The theory of the integrating sphere dictates a diffusely reflecting surface which is Lambertian, and most materials absorb in this region or are specular reflectors. Several salts are commercially available which have high refractive indices and are transparent to wavelengths to 38 microns. Possible coatings are sodium chloride, potassium bromide, potassium chloride, potassium iodide, optical silver chloride, thallium bromide-iodide (KRS-5), lithium fluoride, calcium fluoride, barium fluoride, cesium bromide and cesium iodide. The difficulties in using some of these salts are their water solubilities and the application of them to surfaces as a coating which is diffusely reflective. Flame spraying, sputtering or dispersion in a transparent media are methods of application which might be used. Sublimed flowers of sulfur have been investigated by various workers.

A more accurate and less time consuming measurement of absolute reflectance of magnesium oxide standards may be achieved by placing a two-positioned mirror in the light path into the sphere so that the incoming light could first be focused upon the sphere wall and then upon the test plate (or magnesium oxide standard). This would eliminate the need for a sphere which revolves about the axis, and would make the equalization of the reflectances of the sphere wall and spherical cap standard much easier and more accurate.

APPENDIX I

Error Analysis of the Reflectometer Described in this Report

Absolute Method

The error in the absolute measurement for the cases where $r \neq r_s$ may be computed from Equation 27. Using the values reported in Table I and by letting r equal various values of r_s, the expressions shown below result.

$$r = 0.99r_s, \quad \frac{B_o}{B} = \frac{197.25489 - 194.93957\ r_s}{197.29861 - 193.49014\ r_s} \qquad \text{.....1a}$$

$$r = 1.01r_s, \quad \frac{B_o}{B} = \frac{197.32044 - 198.88049\ r_s}{197.27697 - 197.34578\ r_s} \qquad \text{.....2a}$$

$$r = 0.999r_s, \quad \frac{B_o}{B} = \frac{197.28482 - 196.71210\ r_s}{197.28960 - 195.22641\ r_s} \qquad \text{.....3a}$$

$$r = 1.001r_s, \quad \frac{B_o}{B} = \frac{197.29058 - 197.10378\ r_s}{197.28547 - 195.60922\ r_s} \qquad \text{.....4a}$$

Curves were then obtained by solving Equations 1a through 4a for B_o/B at various values of r_s, and are shown in Figure 11.

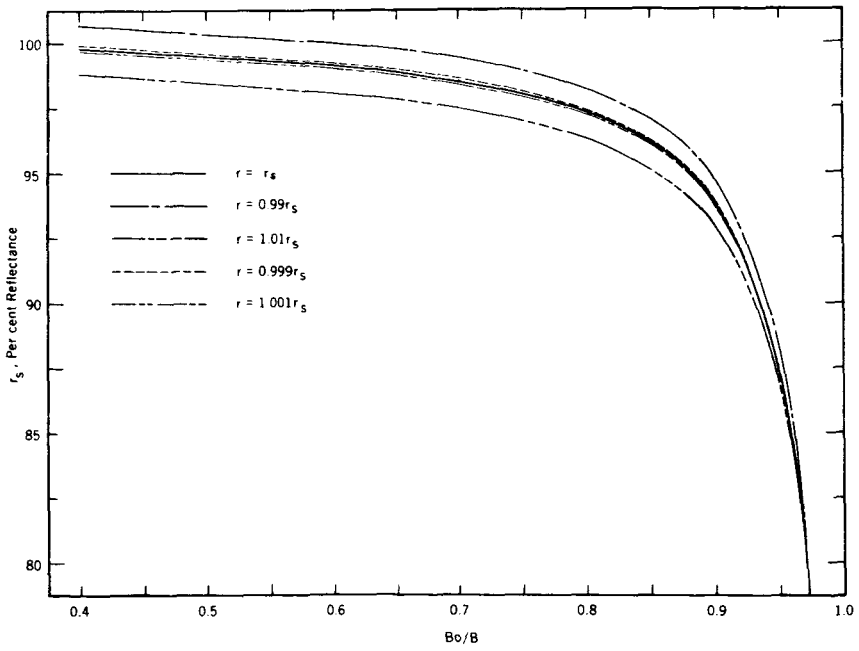

Fig 11 ERRORS IN REFLECTANCE OF MgO STANDARD FOR SEVERAL VALUES OF r/r_s

The reflectances of the spherical cap standard and the sphere wall were made as nearly equal as possible in practice, and were maintained at $r = (1.000 \pm 0.001)r_s$. From Figure 11, it may be seen that the greatest error in our method due to $r_s \neq r$ occurs at high values of reflectance (or, in the visible spectrum), and does not exceed ± 0.001, or $\pm 0.1\%$. This error is negligible below reflectances of 93%. On the other hand, for the case where $r = (1.00 \pm 0.01)r_s$, the error in r_s reaches ± 0.01, or $\pm 1\%$ at high values of reflectance, and is significant throughout the entire range of reflectance values for magnesium oxide.

Comparison Method

Table II lists the calculated errors (from Equation 10) due to the difference in the reflectance of sample and standard for a standard reflectance of 96% and sample reflectances of 94%, 50%, and 10%. It will be noted that this error becomes significant only when measuring the reflectance of black surfaces such as carbon black. The errors in measuring the reflectance by the comparison technique are always positive.

Table II

ERRORS IN MEASUREMENT BY THE COMPARISON TECHNIQUE

Sample Type	Error, α ($r_{st} = 0.96$)		
	Sample Reflectance		
	$r_s = 0.94$	$r_s = 0.50$	$r_s = 0.10$
Spherical	0	0	0
Flat	0	0.003	0.006

APPENDIX II

Error Analysis of a Preston-Type[4] Sphere

Using the same relationships as in the main section of this report, we may derive the wall brightness of a Preston sphere (with flat plate) with a black body at C.

The first reflected flux escaping the sphere is

$$P_1 = rP\left(\frac{C + C_e}{S}\right) . \qquad \ldots\ldots\ldots 5a$$

The multiple reflected flux escaping is

$$P_2 = \pi B_o(C' + C_e - 2CC_e/S) . \qquad \ldots\ldots\ldots 6a$$

The flux received by the rest of the sphere is

$$P' = P + \pi B_o\,(x/r); \qquad \ldots\ldots\ldots 7a$$

therefore, the flux absorbed in the surface is

$$P_3 = (1 - r)(P + \pi B_o x/r). \qquad \ldots\ldots\ldots 8a$$

Since $P = P_1 + P_2 + P_3$, solving for $\pi B_o/P$ after collecting terms results in

$$\frac{\pi B_o}{P} = \frac{r^2}{S}\left[\frac{x}{x(1 - r) + r(C' + C_e - 2CC_e/S)}\right] . \qquad \ldots\ldots\ldots 9a$$

With a test plate of reflectance r_s in place of the black body, the first reflected flux escaping the sphere is

$$P_1 = rPC_e/S. \qquad \ldots\ldots\ldots 10a$$

The multiple reflected flux escaping is

$$P_2 = \pi BC_e. \qquad \ldots\ldots\ldots 11a$$

The flux received by the rest of the sphere is

$$P' = P + \pi B\left(\frac{x}{r} + \frac{C'}{r_s}\right) . \qquad \ldots\ldots\ldots 12a$$

Therefore, the flux absorbed is

$$P_3 = \left[P + \pi B\left(\frac{x}{r} + \frac{C'}{r_s}\right)\right]\left[\frac{(1-r)x}{S - C_e} + \frac{(1-r_s)C'}{S - C_e}\right] \quad \ldots\ldots\ldots 13a$$

Adding Equations 10a, 11a, and 13a, collecting terms and solving for $\pi B/P$, we obtain

$$\frac{\pi B}{P} = \frac{1 - \frac{rC_e}{S} - \frac{(1-r)x}{S - C_e} - \frac{(1-r_s)C'}{S - C_e}}{C_e + \left(\frac{x}{r} + \frac{C'}{r_s}\right)\left(\frac{(1-r)x + (1-r_s)C'}{S - C_e}\right)} \quad \ldots\ldots\ldots 14a$$

Dividing Equation 7a by Equation 14a, we obtain

$$\frac{B_o}{B} = \frac{r^2 x\left[C_e + \left(\frac{x}{r} - \frac{C'}{r_s}\right)\left(\frac{(1-r)s - (1-r_s)C'}{S - C_e}\right)\right]}{S\left[x(1-r) + r\left(C' + C_e - \frac{2CC_e}{S}\right)\right]\left[1 - \frac{rC_e}{S} - \frac{(1-r)x}{S - C_e} - \frac{(1-r_s)C'}{S - C_e}\right]} \quad \ldots\ldots\ldots 15a$$

Assuming a sphere with a radius of 1.95 inches, a sample (test) port of 2.0 inches diameter and exit and entrance ports of 0.70 inch diameters, the following values are obtained:

$$\begin{aligned} S &= 47.78374 \text{ in}^2 \\ C &= 3.38075 \text{ "} \\ C' &= 3.1416 \text{ "} \\ C_e &= 0.77010 \text{ "} \\ x &= 43.62689 \text{ "} \end{aligned}$$

Substituting the above values into Equation 15a, we obtain

$$\frac{B_o}{B} = \frac{r^2\left[0.70859 + \left(\frac{39.83179}{r} + \frac{2.86831}{r_s}\right)\left(0.99502 - 0.92818r - 0.06684r_s\right)\right]}{(43.62689 - 39.81901r)(0.00498 + 0.91194 + 0.06684r_s)} \quad \ldots\ldots\ldots 16a$$

Letting $r = r_s$, Equation 16a reduces to

$$\frac{B_o}{B} = \frac{42.48745r - 41.77886r^2}{0.21726 + 42.50283r - 38.97405r^2} \quad \ldots\ldots\ldots 17a$$

which is plotted in Curve A, Figure 12. Letting $r_s = 1.05r$, Equation 16a reduces to

$$\frac{B_o}{B} = \frac{42.35154r - 41.78512r^2}{0.21726 + 42.84684r - 39.10705r^2} \qquad \ldots\ldots\ldots 18a$$

which is plotted in Curve B, Figure 12.

We note that for $r_s = (1.00 \pm 0.05)r$, the maximum error in r, the reflectance of the sphere wall occurs at lower values of reflectance. The error is approximately 15% at 25% reflectance (true) for $r_s = 1.05r$, and is still 2% at approximately 90% reflectance. The foregoing analysis may be more easily seen if we consider the following: If we assume $r_s = r$, we would read Curve A in Figure 12; while if in reality, $r_s = 1.05r$, we should read Curve B.

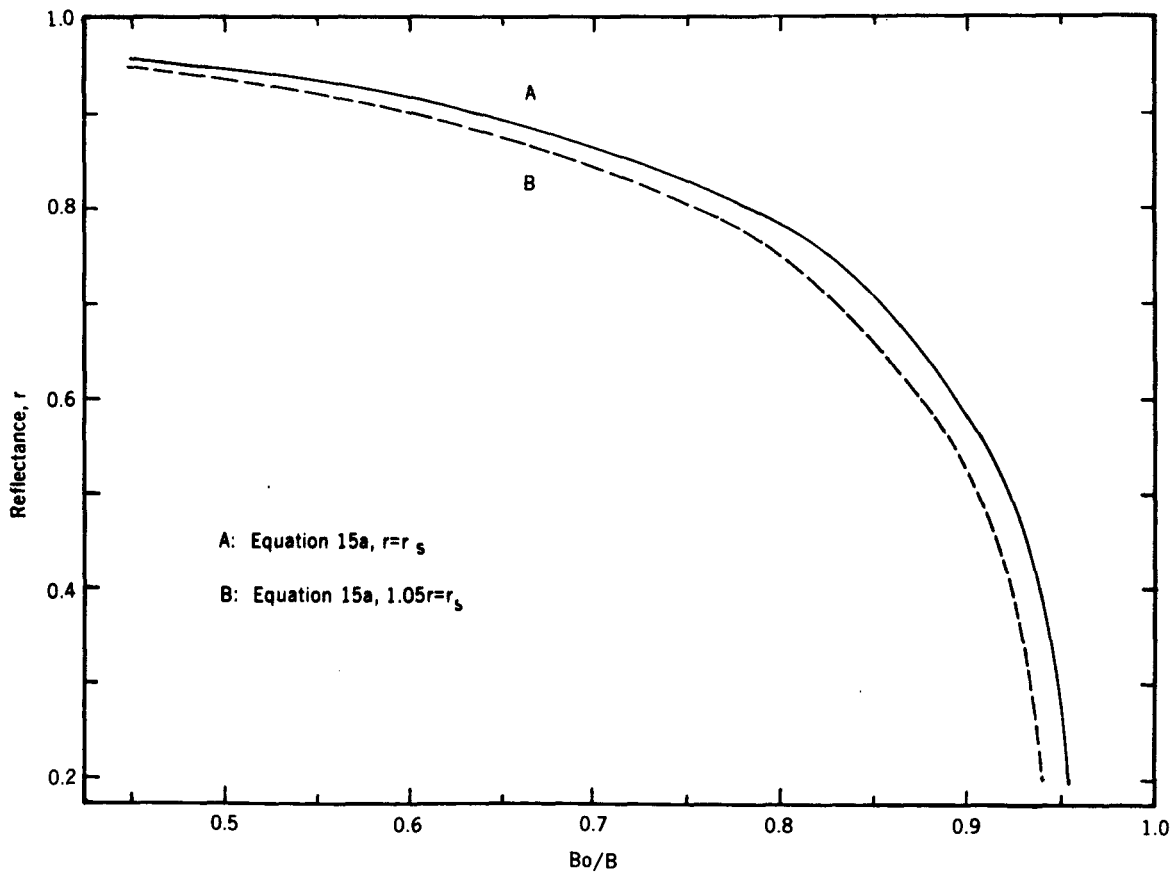

Fig. 12 ERROR IN WALL REFLECTANCE OF A PRESTON SPHERE WHEN $r_s/r = 1.05$

APPENDIX III

The Error Propagated in Measuring the Absolute Reflectance of Unknowns on a Preston-Type Sphere if $r_s = 1.05r$

The infrared reflectances from 1.0 to 3.5 microns were measured under contract for this agency. A Preston sphere of approximately the same dimensions as those noted in Appendix II was used. The following expression was used for obtaining the absolute reflectance of an unknown, r_u;

$$\frac{B_o}{B'} = \frac{x\left[(1 - r)x + r(C' + C_e - 2CC_e/S) - r_u r(C' - C_e(C + C')/S)\right]}{\left[x + r_u C(1 - C_e/S)\right]\left[(1 - r)x + r(C' + C_e - 2CC_e/S)\right]} . \qquad \ldots\ldots\ldots 19a$$

Substituting into Equation 19a, we obtain

$$\frac{B_o}{B'} = \frac{43.62689(43.62689 - 39.81901r - 3.03566r_u r)}{(43.62689 + 3.32585r_u)(43.62689 - 39.81901r)} , \qquad \ldots\ldots\ldots 20a$$

an equation in four variables. Letting $r_u = 0.2$, 0.4, 0.6, and 0.8, Equation 19a reduces to the following equations:

$$r_u = 0.2 \qquad \frac{B_o}{B'} = \frac{1,903.30553 - 1,763.66685r}{1,932.32483 - 1,763.66598r} ; \qquad \ldots\ldots\ldots 21a$$

$$r_u = 0.4 \qquad \frac{B_o}{B'} = \frac{1,903.30553 - 1,790.15413r}{1,961.34413 - 1,790.15239r} ; \qquad \ldots\ldots\ldots 22a$$

$$r_u = 0.6 \qquad \frac{B_o}{B'} = \frac{1,903.30553 - 1,816.64141r}{1,990.36343 - 1,816.63880r} ; \qquad \ldots\ldots\ldots 23a$$

$$r_u = 0.8 \qquad \frac{B_o}{B'} = \frac{1,903.30553 - 1,843.12869r}{2,019.38272 - 1,843.12521r} ; \qquad \ldots\ldots\ldots 24a$$

Equations 21a-24a were then used to determine the effect of an error in the measured sphere reflectance upon the reflectance of an unknown. This was done at four ranges of sphere reflectance by reading the values of r from Curves A and B in Figure 12 for B_o/B values of 0.450, 0.575, 0.725 and 0.875. These values were then substituted into Equations 21a through 24a, and the equations were solved for B_o/B'. The results are tabulated in Table III. The values of r_u versus $B_o B'$ were then plotted and are presented in Figure 13.

The error in the measurement of the reflectance, r_u, of an unknown which results from a positive error (Figure 12) in the determination of the reflectance of the sphere wall due to $r_s = 1.05r$ (idealized as being independent of wavelength) may be seen from examination of Figure 13. The sets of curves (I-IV) represent four ranges of reflectance of the sphere wall (magnesium oxide). Curve A in each case represents the value of r_u for various B_o/B's using Equation 19a according to Preston and as used by the contractor. Curve B represents the values

Table III

ERROR ANALYSIS FOR ABSOLUTE CASE

B_o/B	Curve Fig. 12	r	B_o/B'			
0.450	A	0.960	0.877	0.761	0.647	0.536
	B	0.948	0.889	0.780	0.675	0.573
0.575	A	0.925	0.903	0.810	0.719	0.631
	B	0.910	0.911	0.825	0.742	0.661
0.725	A	0.850	0.933	0.868	0.805	0.744
	B	0.825	0.939	0.880	0.823	0.767
0.875	A	0.650	0.963	0.927	0.893	0.859
	B	0.598	0.967	0.935	0.904	0.873
			0.200	0.400	0.600	0.800
			r_u			

of r_u which should be used if the reflectance of the test plate was 1.05 times that of the sphere wall. Thus, in the case of an unknown with a calculated reflectance of 50% at a wavelength where the calculated reflectance of the sphere wall is 92.5%, the true reflectance of the sphere may be read from Curve B, Figure 12, while that of the unknown may be read from Curve II-B, Figure 13. (Figure 13 should show a great number of sets of curves corresponding to the entire reflectance

range of the MgO coated sphere wall, but for simplicity, only four sets were calculated). The true absolute reflectance of the above unknown would be determined by reading r_u from Curve II-B, Figure 13, at a B_o/B' value corresponding to $r_u = 50\%$ on Curve II-A, and is in this case 55%, a negative error of 5% absolute reflectance (where $B_o/B' = 0.7625$). The sphere wall's reflectance would be 91.0% rather than 92.5%, or a positive error of 1.5%.

Similarly, for r = 96.0% and an unknown of 80%, the true value of r would be 94.8% or a positive error of 1.2%; and the true reflectance of the unknown would be 87.5%, a negative error of 7.5% (from Curves II-A and II-B, Figure 13).

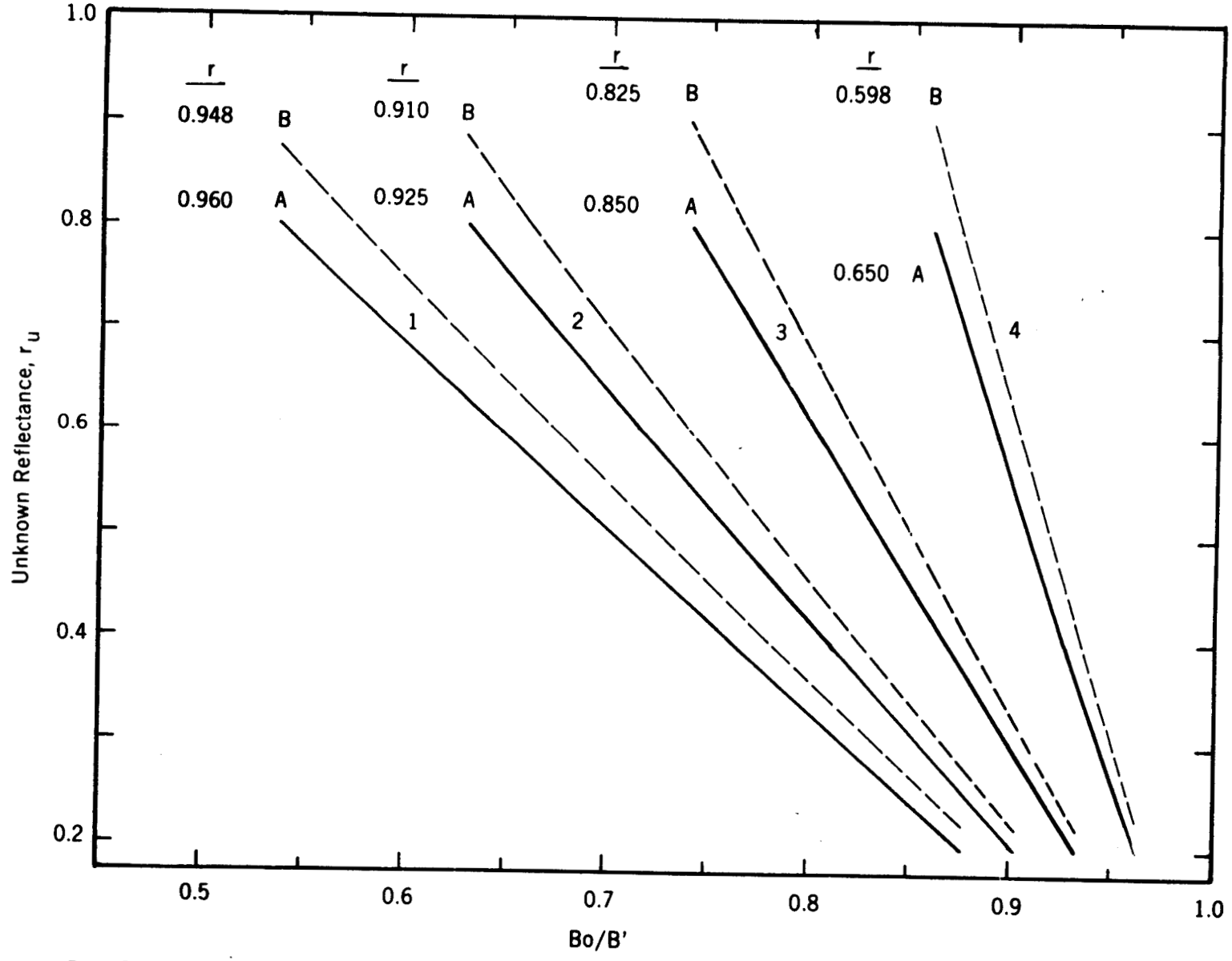

Fig. 13 ERROR IN REFLECTANCES OF UNKNOWNS ON A PRESTON SPHERE WHEN r / rs = 1.05

REFERENCES

1. H. J. McNickolas, Bur. Standards J. Research, 1, 29, (1928)

2. E. Karrer, Sci. Papers, Bur. Standards, No. 415, 203 (1921)

3. A. H. Taylor, J. Opt. Soc. America, 4, 9 (1920)

4. J. S. Preston, Trans. Opt. Soc. (London), 31, 15 (1929-30)

5. W. E. K. Middleton and C. L. Sanders, J. Opt. Soc. Am., 41, 419 (1951)

6. P. A. Tellex and J. R. Waldron, J. Opt. Soc. Am., 45, 1, 19 (1955)

7. J. A. Jacquez and H. F. Kuppenheim, J. Opt. Soc. Am., 45, 6, 460 (1955)

8. Nat. Bur. Standards (U.S.) Lttr. Circ. LC547, March 17, 1939

9. H. T. Betz et al, Armour Research Foundation, WADC TR 56-222, Part II, October 1958

10. National Bureau of Standards

APPROVED: MTP-M-S&M-M-60-6

J. R. NUNNELLEY
Chief, Analytical Chemistry Section

D. B. FRANKLIN
Chief, Corrosion & Physical Chemistry Section

W. R. LUCAS
Chief, Engineering Materials Branch

W. A. MRAZEK
Director, Structures & Mechanics Division

DISTRIBUTION:

M-DIR
M-S&M-DIR
M-S&M-P
M-S&M-M (10)
M-S&M-MA (4)
M-S&M-MC (4)
M-MS-IP (8)
M-RP-T
Attn: Messrs Heller, Snoddy,
Gates and Dr. Schocken
M-G&C-M